

# Path planning and reactive based control for a quadrotor with a suspended load

José J. Corona-Sánchez<sup>1</sup>, Raymond Kristiansen<sup>2</sup> and Tom Stian Andersen<sup>3</sup>

**Abstract**—This paper presents a solution to quadrotor cargo transportation, more precisely when cargo is suspended as a sling load. The challenge lies in payload position control and swing attenuation, which we approach by dividing the model into subsystems: attitude quadrotor in free flight, and translational and attitude load dynamics. We propose a solution based on reactive control, in the sense that we utilize a reactive force that reacts to the error position and the oscillation in the load. Asymptotic stability of the system's closed-loop equilibrium is proved using Lyapunov theory. Additionally, a three-dimensional path planning algorithm is proposed based on cubic splines, which give us a natural path between initial and final desired points. Moreover, we convert the path planning problem into trajectory tracking with a spline's correct parametrization. Control and path planning performance are demonstrated with numerical simulations in three different scenarios.

## I. INTRODUCTION

The modern world experiences a growing use of robots to perform specific tasks. Unmanned aerial vehicles (UAV) in particular have seen a significant technology advance wherewith it is possible to find many applications, e.g., monitoring and inspection, aerial photography, and package delivery.

The UAV applications era is now with us; thus, it is essential to propose simple solutions to daily activities. Transporting cargo is one of the most versatile tasks that a UAV can manage. A common approach is to carry such cargo as a suspended sling load connected to a quadrotor with a cable. Cargo transportation is not a new problem and has been studied in earlier works. For example, [1] derives cable-suspended load equations of motion for quadrotors using the Lagrange method and presents control design specialized to the planar case, tracking of either the quadrotor attitude, the load attitude, or the position of the load. Another approach is presented in [2], where the Euler-Lagrange formulation is used to obtain the dynamic model of the system, integrating the dynamics of quadrotor, cable, and payload. Two cases are considered to develop two different control laws, dependent or independent of the payload's swing angle. In [3], the

dynamic model is developed using Newton-Euler formulation, which is further verified and compared to a model based on the Lagrange approach. A nonlinear control strategy based on the dynamic model is designed to control the quadrotor's position and attitude. A passivity-based approach is employed in [4], based on a model developed using the Euler-Lagrange formulation. Moreover, the paper develops an Interconnection and Damping Assignment-Passivity Based Control (IDA-PBC) for a quadrotor UAV transporting a cable-suspended payload.

In the previous references, the complete dynamic system is considered to develop the mathematical models, and it can be observed that the rotational quadrotor movement is independent of the load dynamics when the load is connected to the quadrotor's center of gravity. This fact is exploited in other works. For example, in [5], the load is modelled as a pendulum with a rigid link, and the interconnected system is modelled by Kane's method [6]. A nonlinear controller is derived using the backstepping technique, which ensures trajectory tracking of the UAV regardless of the pendulum motion. Another example to model the entire dynamic system as two connected subsystems is showed in [7]. The subsystems are the suspended load dynamics and the free-flight quadrotor attitude. A trajectory tracking controller for the load position is then designed based on existing Lyapunov-based trajectory tracking. The authors in [8] present a nonlinear controller synthesis to deal with a quadrotor's trajectory tracking problem with a suspended load constrained to flight on a plane. The control design is a saturated controller for the vertical dynamics, and a backstepping controller is derived in order to synthesize the resulting closed-loop dynamics.

The problem of controlling a quadrotor with a suspended load may be roughly divided into two categories: either make sure that the quadrotor follows its desired trajectory without influence of the load (i.e. controlling the quadrotor), or ensure that the load follows a desired trajectory by quadrotor actuation (i.e. controlling the load). The main idea of this work is to focus on the latter, ensuring cargo transportation between constant positions. Thus we aim for a powerful control strategy that also is simple to implement, where a suitable approach is reactive control. Reactive-based control has been used to control quadrotors previously; for instance, [9] presents a reaction-based control where the attitude subsystem reacts to errors in the translational motion. The strength in this methodology lies in no requirement of generating the desired attitude or angular velocity. Also, in [10], a second-order sliding mode attitude controller is

\*This research was funded by the Norwegian Research Council and is part of the project 282317: Sikrere logistikk fra fartøy med ubemannet logistikkhelikopter.

<sup>1</sup>José J. Corona-Sánchez is with the Department of Electrical Engineering, UiT The Arctic University of Norway, 8515 Narvik, Norway jose.j.sanchez@uit.no

<sup>2</sup>Raymond Kristiansen is with the Department of Electrical Engineering, UiT The Arctic University of Norway, 8515 Narvik, Norway raymond.kristiansen@uit.no

<sup>3</sup>Tom Stian Andersen is with the Department of Electrical Engineering, UiT The Arctic University of Norway, 8515 Narvik, Norway tom.s.andersen@uit.no

derived which exponentially stabilizes the attitude at hover, and a PD controller for translational error is used to inject angular accelerations into the rotational dynamics. In this paper, we follow the ideas developed in [9], which computes the total necessary force to move and reduce the load's oscillations without controlling the swing angles but inject damping in the angular swinging velocity. More precisely, swing attenuation is performed in the plane projections ( $xz^n$  and  $yz^n$ ) of the swing angles, setting a non-restrictive control over the swing angles.

After the control strategy is defined, it is necessary to develop a path planning approach to execute the task safely, of which several algorithms are available in the literature. For example, [11] presents a survey of two-dimensional geometric path planning algorithms for a fixed-wing. In [12] path-following using Line-of-Sight (LOS) guidance in 2D is thoroughly analyzed and solved in the ideal case of no disturbances. It also shows how 3D path-following can be divided into horizontal and vertical planes, effectively reducing the 3D path following problem into two 2D path-following problems. Approaches to the specific path planning of cargo transportation can be found in [13], where an input shaped trajectory generation is proposed as an effective way to minimize post-flight swinging for rest-to-rest maneuvers by allowing some swinging motions during flight. A controller is developed to track these shaped trajectories and permit the associated payload swinging while also rejecting unwanted swinging disturbances. The path planner and controller are implemented in simulation. The authors in [14] present a trajectory planning method based on predictive control, and the cost function considering load swing angle and distance between obstacle and UAV is designed to generate an optimal trajectory. Simulations show that the proposed methods can minimize the swing angle and avoid obstacles at the level of the desired trajectory.

The central problem in this paper is to move the cargo from point A to point B, and thus, a path built by point interpolation can be used. Spline interpolation gives us a powerful tool to solve this task. Some previous works exploit spline's capability; for instance, in [15] the authors develop a three-dimensional guidance strategy for fixed-wing UAVs using quaternions. The guidance algorithm based on Hermite splines is applied to a simple kinematic model for a fixed-wing UAV with a simple kinematic controller. This work's contribution on path planning is a three-dimensional strategy based on cubic splines that interpolates a set of points chosen in strategic form. This makes up a significant difference with previous works in the sense that the selected path is parameterized to build the desired trajectory, converting the path planning problem into trajectory tracking one.

This paper is organized as follows: The mathematical model of the payload and translational motion of the quadrotor is developed in Section II, while Section III develops the control law as well as a stability analysis using Lyapunov theory. The path planning strategy is described in Section IV, while Section V presents three numerically simulated scenarios to demonstrate control and path planning performance.

Finally, conclusions are given in Section VI.

## II. DYNAMIC MODEL

### A. Notation and coordinate reference frames

Throughout this paper, scalar values are denoted in normal face, vectors in boldface, while matrices are written in capital boldface letters. The time derivative is denoted as  $\dot{\mathbf{x}} = \frac{d\mathbf{x}}{dt}$ , such that  $\ddot{\mathbf{x}} = \frac{d^2\mathbf{x}}{dt^2}$ . The Euclidean norm is denoted by  $\|\cdot\|$  and  $|\cdot|$  denotes the absolute value. Vectors are decomposed in different reference frames denoted by superscripts, where  $\mathcal{F}^n$  denotes the inertial frame, while  $\mathcal{F}^b$  denotes the body frame, as shown in Figure 1.

### B. Dynamic model of a rigid body with a suspended load

We consider a rigid body with a suspended load, as shown in Figure 1, with a total of eight degrees of freedom. We assume that the cable is connected to the gravity center of the quadrotor, such that the load does not affect the body rotational dynamics, similar to the approach in [4], [1]. Thus, the whole system can be divided into subsystems: 1) rotational quadrotor dynamics (3DOF) and 2) translational and rotational motion of the load (5DOF). We develop our model based on the Euler-Lagrange method, where we first consider the following assumptions:

- The cable is rigid with a negligible mass.
- The payload is considered as a mass point.
- The aerodynamic effects are neglected.

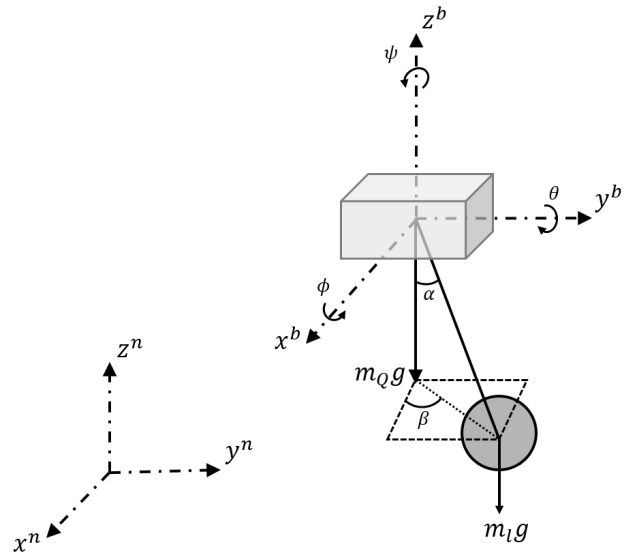


Fig. 1. Rigid body with a cable-suspended payload

Further, we proceed by defining the generalized coordinates as  $\mathbf{g}_c = [\mathbf{p}_q^n \mathbf{r}]^\top$ , where  $\mathbf{p}_q^n = [x_q \ y_q \ z_q]^\top$  is the position of the rigid body with respect to the inertial frame, and  $\mathbf{r}$  is the unit vector aligned with the cable connecting the quadrotor to the load. Notice that the vector  $\mathbf{r}$  has the

non-holonomic constraint  $\|\mathbf{r}\| = 1$ , which can be put in the form

$$f_\delta(q_1, \dots, q_n; \dot{q}_1, \dots, \dot{q}_n) = 0 \quad (1)$$

where the index  $\delta = 1, 2, \dots, i$  indicate the number of constraint equations. We need to include the constraint in the Lagrange equations of motion and use the Lagrange multipliers method to eliminate the extra virtual degree of freedom [16]. The kinematic and potential energy of quadrotor and load are

$$\begin{aligned} T_q &= \frac{1}{2} m_q \mathbf{V}_q^{\text{n}\top} \mathbf{V}_q^{\text{n}} & V_q &= m_q g \mathbf{e}_3^\top \mathbf{p}_q^{\text{n}} \\ T_l &= \frac{1}{2} m_l \mathbf{V}_l^{\text{n}\top} \mathbf{V}_l^{\text{n}} & V_l &= m_l g l \mathbf{e}_3^\top \mathbf{p}_l^{\text{n}} \end{aligned}$$

where  $\mathbf{V}_q^{\text{n}}$  is the quadrotor velocity,  $\mathbf{V}_l^{\text{n}}$  is the linear velocity of the load,  $\mathbf{e}_3 = [0, 0, 1]^\top$ ,  $g$  is the gravity acceleration,  $l$  is the cable length,  $m_q$  is the quadrotor mass and  $m_l$  is the load mass. It is important to note that we are not considering the quadrotor attitude, because the load is attached in the quadrotor's gravity center. Further, we can write the load position and velocity as

$$\begin{aligned} \mathbf{p}_l^{\text{n}} &= \mathbf{p}_q^{\text{n}} + l\mathbf{r} \\ \mathbf{V}_l^{\text{n}} &= \mathbf{V}_q^{\text{n}} + l\dot{\mathbf{r}}. \end{aligned} \quad (2)$$

Thus, the Lagrangian in terms of the quadrotor movement can be written as

$$\begin{aligned} L &= \frac{1}{2} (m_q + m_l) \mathbf{V}_q^{\text{n}\top} \mathbf{V}_q^{\text{n}} + l m_l \mathbf{V}_q^{\text{n}\top} \dot{\mathbf{r}} + \frac{1}{2} l^2 m_l \dot{\mathbf{r}}^\top \dot{\mathbf{r}} \\ &- (m_q + m_l) g \mathbf{e}_3^\top \mathbf{p}_q^{\text{n}} - m_l g l \mathbf{e}_3^\top \mathbf{r}. \end{aligned} \quad (3)$$

Applying the Euler-Lagrange methodology, we obtain

$$\begin{aligned} m \dot{\mathbf{V}}_q^{\text{n}} + l m_l \ddot{\mathbf{r}} + m g \mathbf{e}_3 &= \mathbf{f}^{\text{n}} \\ \mathbf{r} \times \left( l m_l \dot{\mathbf{V}}_q^{\text{n}} + l^2 m_l \ddot{\mathbf{r}} + l m_l g \mathbf{e}_3 \right) &= \mathbf{r} \times (l \mathbf{f}^{\text{n}} + \mathbf{Q}_k) \end{aligned} \quad (4)$$

which represent the rotational and translational dynamics of the payload, where  $\mathbf{f}^{\text{n}}$  is the external force in inertial frame,  $m = m_q + m_l$  is the total mass and  $\mathbf{Q}_k$  is a function due to the constraint presented by [16], i.e.

$$\mathbf{Q}_k = \sum_{\delta=1}^i \left\{ \lambda_\delta \left[ \frac{\partial f_\delta}{\partial q_k} - \frac{d}{dt} \left( \frac{\partial f_\delta}{\partial \dot{q}_k} \right) \right] - \frac{d\lambda_\delta}{dt} \frac{\partial f_\delta}{\partial \dot{q}_k} \right\}.$$

Now, rewriting the constraint in the form of (1) we have  $r_1^2 + r_2^2 + r_3^2 - 1 = 0$ , therefore  $\mathbf{Q}_k = 2\lambda \mathbf{r}$ , where  $\lambda$  is the Lagrange multiplier. There is only one multiplier because the system has one constraint.

The control objective is cargo transportation, so it is essential to minimize the oscillations and control the cargo position; hence, it is convenient to represent the translational and rotational dynamic model in terms of the load position, velocity, and acceleration. Using the identities in (2), substituted into (4), we obtain

$$\begin{aligned} (m_q + m_l) \dot{\mathbf{V}}_l^{\text{n}} - l m_q \ddot{\mathbf{r}} + g (m_q + m_l) \mathbf{e}_3 &= \mathbf{f}^{\text{n}} \\ \mathbf{r} \times \left( l m_q \dot{\mathbf{V}}_l^{\text{n}} - l^2 m_q \ddot{\mathbf{r}} + l g m_q \mathbf{e}_3 - l \mathbf{f}^{\text{n}} - 2\lambda \mathbf{r} \right) &= 0 \end{aligned} \quad (5)$$

which we may combine to establish the relation

$$-\mathbf{r} \times (l^2 m_q \ddot{\mathbf{r}} + l \mathbf{f}^{\text{n}}) = 0.$$

On the other hand, the first equation of (5) can be simplified using

$$\begin{aligned} \frac{d}{dt} (\dot{\mathbf{r}} \cdot \dot{\mathbf{r}}) &= 0 \\ \mathbf{r} \times (\mathbf{r} \times \ddot{\mathbf{r}}) &= \mathbf{r} (\mathbf{r} \ddot{\mathbf{r}}) - \ddot{\mathbf{r}} (\mathbf{r} \mathbf{r}) = -(\dot{\mathbf{r}} \dot{\mathbf{r}}) \mathbf{r} - \ddot{\mathbf{r}} \\ \ddot{\mathbf{r}} &= -(\dot{\mathbf{r}} \dot{\mathbf{r}}) \mathbf{r} - \mathbf{r} \times (\mathbf{r} \times \ddot{\mathbf{r}}) \end{aligned}$$

and finally, defining  $\dot{\omega} = \mathbf{r} \times \ddot{\mathbf{r}}$ , we obtain the dynamics equations

$$\begin{aligned} (m_q + m_l) (\dot{\mathbf{V}}_l^{\text{n}} + g \mathbf{e}_3) &= [\mathbf{r} \mathbf{f}^{\text{n}} - l m_q (\dot{\mathbf{r}} \cdot \dot{\mathbf{r}})] \mathbf{r} \\ l m_q \dot{\omega} &= -\mathbf{r} \times \mathbf{f}^{\text{n}}. \end{aligned} \quad (6)$$

Moreover, from circular motion, the kinematic is defined by

$$\dot{\mathbf{r}} = \omega \times \mathbf{r}. \quad (7)$$

### C. Attitude Quadrotor Model

We assume that the load is connected in the quadrotor center of gravity, so it does not influence the quadrotor attitude movement. Following [17], we apply quaternions to parametrize attitude, with kinematics and dynamics given by

$$\begin{aligned} \dot{\mathbf{q}}_{\text{n,b}} &= \frac{1}{2} \Omega_{\text{n,b}}^{\text{n}} \otimes \mathbf{q}_{\text{n,b}} = \frac{1}{2} \mathbf{q}_{\text{n,b}} \otimes \Omega_{\text{n,b}}^{\text{b}} \\ \dot{\Omega}_{\text{n,b}}^{\text{b}} &= (\mathbf{J}^{\text{b}})^{-1} (\tau^{\text{b}} - \Omega_{\text{n,b}}^{\text{b}} \times (\mathbf{J}^{\text{b}} \Omega_{\text{n,b}}^{\text{b}})) \end{aligned} \quad (8)$$

where  $\mathbf{q}_{\text{n,b}} = [q_0, q_1, q_2, q_3]^\top$  is the unit quaternion that rotates from  $\mathcal{F}^{\text{n}}$  to  $\mathcal{F}^{\text{b}}$ ,  $\Omega_{\text{n,b}}^{\text{b}}$  is the angular body velocity represented in  $\mathcal{F}^{\text{b}}$ ,  $\mathbf{J}^{\text{b}} = \text{diag}\{J_x, J_y, J_z\}$  is the quadrotor inertia matrix, and  $\tau^{\text{b}}$  is the quadrotor torques produced by the rotors.

## III. REACTIVE CONTROL

In this paper, the main objective is to transport cargo and reduce the oscillations in the load, and it is possible to work first with the equations in (6), which represent translational and attitude load dynamics. Hence, we divide the control law into tasks: 1) Compute a force that drives the translational load error to zero, reduces the load oscillations, and guarantee asymptotically stability. 2) With the total force described in the first task, control the quadrotor movement with a control law similar to [9].

### A. Reactive Force

Rewriting with the second equation of (6), we obtain

$$\dot{\omega} = \mathbf{r} \times \ddot{\mathbf{r}} = \begin{bmatrix} \dot{\omega}_x \\ \dot{\omega}_y \\ \dot{\omega}_z \end{bmatrix} = -\frac{1}{lm_q} (\mathbf{r} \times \mathbf{f}^n)$$

as the angular acceleration of the swing angles projected in the different planes  $xz^n$ ,  $yz^n$ , and  $xy^n$ , cf. Figure 2. With this in mind, we can establish a control law for the planes  $xz^n$  and  $yz^n$ . For our purpose, the  $xy^n$  plane does not need to be controlled since this action is redundant of the other planes. The new control problem is then as in Figure 3.

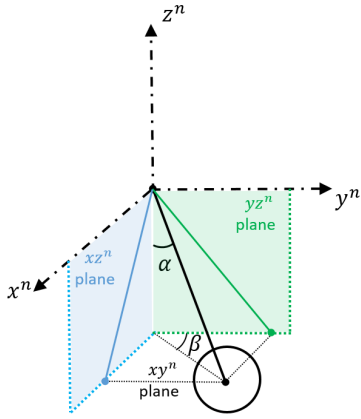


Fig. 2. Swing load projections in the planes

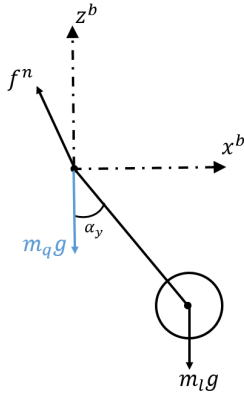


Fig. 3. Swing load plane  $xz^n$

We define the load errors as

$$\begin{aligned} x_e &= x - x_d; & \dot{x}_e &= V_{l_x}^n - \dot{x}_d; & \ddot{x}_e &= \dot{V}_{l_x}^n - \ddot{x}_d \\ z_e &= z - z_d; & \dot{z}_e &= V_{l_z}^n - \dot{z}_d; & \ddot{z}_e &= \dot{V}_{l_z}^n - \ddot{z}_d \end{aligned}$$

and consider  $\mathbf{f}^n = [f_x^n, f_y^n, f_z^n]^T = \mathbf{q}_{n,b} \otimes [0 \ 0 \ 0 \ T]^T \otimes \mathbf{q}_{n,b}^*$ , where  $T$  is the thrust produced by the quadrotor. We can expand the first equation of (6) as

$$\dot{\mathbf{V}}_1^n = \frac{1}{m} [r_1 f_x^n + r_2 f_y^n + r_3 f_z^n - lm_q (\dot{\mathbf{r}} \cdot \dot{\mathbf{r}})] \mathbf{r} - g \mathbf{e}_3.$$

Now, considering the force in the plane  $xz^n$  solely, we have

$$\dot{\mathbf{V}}_{1xz}^n = \frac{1}{m} (r_1 f_x^n + r_3 f_z^n - lm \|\dot{\mathbf{r}}\|^2) \begin{bmatrix} r_1 \\ r_3 \end{bmatrix} - \begin{bmatrix} 0 \\ g \end{bmatrix}.$$

Further, we define control forces  $f_x^n$  and  $f_z^n$  as

$$\begin{aligned} f_x^n &= m (k_\omega \omega_y + k_{p_x} x_e + k_{d_x} \dot{x}_e + r_1 g + \ddot{x}_d) \\ &\quad + r_1 lm_q \|\dot{\mathbf{r}}\|^2 \end{aligned} \quad (9)$$

$$f_z^n = m (k_{p_z} z_e + k_{d_z} \dot{z}_e + g + \ddot{z}_d) + r_3 lm_q \|\dot{\mathbf{r}}\|^2$$

with  $k_{p_x}$ ,  $k_{d_x}$ ,  $k_{p_z}$ ,  $k_{d_z}$ ,  $k_\omega$  as controller gains. Notice that the  $k_\omega \omega_y$  is the damping term to minimize the oscillations, in this case the oscillations around  $y^n$  axis. Hence, we obtain

$$\begin{aligned} \dot{\mathbf{V}}_{1xz}^n &= \begin{bmatrix} r_1^2 (k_\omega \omega + k_{p_x} x_e + k_{d_x} \dot{x}_e) + r_1 (r_1^2 + r_3) g \\ r_3^2 (k_{p_z} z_e + k_{d_z} \dot{z}_e) + (r_1^2 r_3 + r_3^2 - 1) g \end{bmatrix} \\ &\quad + \begin{bmatrix} r_1 r_3 (k_{p_z} z_e + k_{d_z} \dot{z}_e) \\ r_1 r_3 (k_\omega \omega + k_{p_x} x_e + k_{d_x} \dot{x}_e) \end{bmatrix} \\ &\quad + \begin{bmatrix} (r_1^2 - 1) \ddot{x}_d + r_1 r_3 \ddot{z}_d \\ (r_3^2 - 1) \ddot{z}_d + r_1 r_3 \ddot{x}_d \end{bmatrix} \end{aligned}$$

$$\begin{aligned} \dot{\omega}_y &= m_t (r_1 (k_{p_z} z_e + k_{d_z} \dot{z}_e) + r_1 (1 + r_3) g) \\ &\quad - m_t r_3 (k_\omega \omega + k_{p_x} x_e + k_{d_x} \dot{x}_e) \\ &\quad + m_t (r_3 \ddot{x}_d + r_1 \ddot{z}_d) \end{aligned}$$

with  $m_t = \frac{m}{m_q l}$ . More compactly, we write

$$\dot{\tilde{\mathbf{X}}} = \mathbf{A} \tilde{\mathbf{X}} + \mathbf{g}_1(\tilde{\mathbf{X}}) + \mathbf{g}_2(\tilde{\mathbf{X}}) + \mathbf{G}_d + \mathbf{g}_3(\ddot{\mathbf{X}}_d)$$

where

$$\begin{aligned} \tilde{\mathbf{X}} &= \begin{bmatrix} x_e \\ \dot{x}_e \\ z_e \\ \dot{z}_e \\ \omega_y \end{bmatrix}; & \mathbf{G}_d &= \begin{bmatrix} 0 \\ r_1 (r_1^2 + r_3) g \\ 0 \\ (r_1^2 r_3 + r_3^2 - 1) g \\ m_t r_1 (1 + r_3) g \end{bmatrix} \\ \mathbf{g}_1(\tilde{\mathbf{X}}) &= \begin{bmatrix} 0 \\ r_1 r_3 (k_{p_z} z_e + k_{d_z} \dot{z}_e) + r_1^2 k_\omega \omega_y \\ 0 \\ r_1 (k_\omega \omega_y + k_{p_x} x_e + k_{d_x} \dot{x}_e) \\ m_t r_1 (k_{p_z} z_e + k_{d_z} \dot{z}_e) \end{bmatrix} \\ \mathbf{g}_2(\tilde{\mathbf{X}}) &= \begin{bmatrix} 0 \\ -r_3^2 (k_\omega \omega_y + k_{p_x} x_e + k_{d_x} \dot{x}_e) \\ 0 \\ 0 \\ 0 \end{bmatrix} \\ \mathbf{g}_3(\ddot{\mathbf{X}}_d) &= \begin{bmatrix} 0 \\ (r_1^2 - 1) \ddot{x}_d + r_1 r_3 \ddot{z}_d \\ 0 \\ (r_3^2 - 1) \ddot{z}_d + r_1 r_3 \ddot{x}_d \\ m_t (r_3 \ddot{x}_d + r_1 \ddot{z}_d) \end{bmatrix} \end{aligned}$$

$$\mathbf{A} = \begin{bmatrix} 0 & 1 & 0 & 0 & 0 \\ k_{p_x} & k_{d_x} & 0 & 0 & 0 \\ 0 & 0 & 0 & 1 & 0 \\ 0 & 0 & r_3^2 k_{p_z} & r_3^2 k_{d_z} & 0 \\ -m_t r_3 k_{p_x} & -m_t r_3 k_{d_x} & 0 & 0 & -m_t r_3 k_\omega \end{bmatrix}.$$

## B. Lyapunov Stability

Before we proceed with the stability analysis, we assume that the  $\mathbf{r}$  unit vector is bounded with  $r_1, r_2 \in (-1, 1)$  and  $r_3 \in (0, -1]$ , hence, we reasonably assume that the load will always be maintained below the quadrotor. Define a Lyapunov function candidate as

$$V(\tilde{\mathbf{X}}) = \tilde{\mathbf{X}}^\top \mathbf{P} \tilde{\mathbf{X}}$$

where  $\mathbf{P}$  is a positive definite symmetric matrix. Moreover, if  $\mathbf{A}$  is Hurwitz there exists

$$-\mathbf{Q} = \mathbf{P}\mathbf{A} + \mathbf{A}^\top \mathbf{P}$$

with  $\mathbf{Q}$  positive definite and symmetric. The demonstration of  $\mathbf{A}$  being Hurwitz is developed in the appendix. The time derivative of  $V(\tilde{\mathbf{X}})$  is then

$$\begin{aligned} \dot{V}(\tilde{\mathbf{X}}) &= -\tilde{\mathbf{X}}^\top \mathbf{Q} \tilde{\mathbf{X}} + 2\tilde{\mathbf{X}}^\top \mathbf{P} \left[ \mathbf{g}_1(\tilde{\mathbf{X}}) + \mathbf{g}_2(\tilde{\mathbf{X}}) \right] \\ &\quad + 2\tilde{\mathbf{X}}^\top \mathbf{P} \left[ \mathbf{G}_d + \mathbf{g}_3(\tilde{\mathbf{X}}_d) \right]. \end{aligned} \quad (10)$$

The first term on the right-hand side is negative definite, while the other terms are sign indefinite. Furthermore, due to the bounds in  $\mathbf{r}$  all products between the components of  $\mathbf{r}$  in  $\mathbf{g}_1(\tilde{\mathbf{X}})$  and  $\mathbf{g}_2(\tilde{\mathbf{X}})$  can be upper bounded by one, i.e.

$$\begin{bmatrix} r_1^2 \\ r_1 \\ r_1 r_3 \\ r_3^2 \end{bmatrix} \leq 1$$

thus

$$\begin{aligned} \mathbf{g}_1(\tilde{\mathbf{X}}) &\leq \left\| \begin{bmatrix} 0 \\ k_{p_z} z_e + k_{d_z} \dot{z}_e + k_\omega \omega_y \\ 0 \\ k_\omega \omega_y + k_{p_x} x_e + k_{d_x} \dot{x}_e \\ m_t (k_{p_z} z_e + k_{d_z} \dot{z}_e) \end{bmatrix} \right\| \\ \mathbf{g}_2(\tilde{\mathbf{X}}) &\leq \left\| \begin{bmatrix} 0 \\ -(k_\omega \omega_y + k_{p_x} x_e + k_{d_x} \dot{x}_e) \\ 0 \\ 0 \\ 0 \end{bmatrix} \right\|. \end{aligned}$$

Defining  $\mathbf{g}(\tilde{\mathbf{X}}) = \mathbf{g}_1(\tilde{\mathbf{X}}) + \mathbf{g}_2(\tilde{\mathbf{X}})$ , which satisfies

$$\frac{\|\mathbf{g}(\tilde{\mathbf{X}})\|}{\|\tilde{\mathbf{X}}\|} \rightarrow c \quad \text{as} \quad \|\tilde{\mathbf{X}}\| \rightarrow 0$$

and therefore, there exists  $\gamma > 0$  such that

$$\|\mathbf{g}(\tilde{\mathbf{X}})\| < \gamma \|\tilde{\mathbf{X}}\| \leq \gamma \|\tilde{\mathbf{X}}\|^2.$$

Consequently, the second term of (10) can be bounded as

$$2\tilde{\mathbf{X}}^\top \mathbf{P} \mathbf{g}(\tilde{\mathbf{X}}) \leq 2\gamma \|\mathbf{P}\| \|\tilde{\mathbf{X}}\|^2.$$

Additionally, it is straight forward to show that the third term of (10) can be bounded as

$$2\tilde{\mathbf{X}}^\top \mathbf{P} \mathbf{G}_d \leq 2\kappa g \sqrt{2 + m_t^2} \|\mathbf{P}\| \|\tilde{\mathbf{X}}\|^2$$

where  $\kappa > 0$  satisfies

$$\begin{bmatrix} r_1 (r_1^2 + r_3) \\ r_1^2 r_3 + r_3^2 - 1 \\ r_1 (1 + r_3) \end{bmatrix} < \kappa.$$

The last term of (10) can be bounded as

$$2\tilde{\mathbf{X}}^\top \mathbf{P} \mathbf{g}_3(\tilde{\mathbf{X}}_d) \leq 2\sqrt{2 + m_t^2} \|\mathbf{P}\| \|\tilde{\mathbf{X}}\|^2 h(t)$$

with  $h(t) = |\ddot{x}_d| + |\ddot{z}_d|$ . Therefore,  $\dot{V}(\tilde{\mathbf{X}})$  satisfies

$$\dot{V}(\tilde{\mathbf{X}}) \leq -[\lambda_{\min}(\mathbf{Q}) - 2(\Gamma + k_m h(t)) \|\mathbf{P}\|] \|\tilde{\mathbf{X}}\|^2 \quad (11)$$

where  $\Gamma = \kappa g k_m + \gamma$  and  $k_m = \sqrt{2 + m_t^2}$ . Hence, selecting

$$h(t) < \frac{1}{k_m} \left( \frac{\lambda_{\min}(\mathbf{Q})}{2\|\mathbf{P}\|} - \Gamma \right)$$

ensures that  $\dot{V}(\tilde{\mathbf{X}})$  is negative definite. Thus, all the conditions of Theorem 4.10 in [18] are satisfied for  $-1 \leq r_1 \leq 1$ ,  $-1 \leq r_2 \leq 1$  and  $-1 \leq r_3 \leq 0$ , and we conclude that the origin of the closed loop system is asymptotically stable.

## C. Controlling the $yz^n$ plane

The control law for the  $yz^n$  plane can be obtain in the same way as for  $xz^n$  control. Thus, the reactive force  $f_y^n$  can be proposed as

$$f_y^n = m(k_\omega \omega_x + k_{p_x} y_e + k_{d_y} \dot{y}_e + r_2 g) + r_2 l m_q \|\dot{\mathbf{r}}\|^2 \quad (12)$$

where  $y_e = y - y_d$  is the position error in the  $y^n$  axis, and  $f_z^n$  as in (9). Since  $f_y^n$  has the same structure as  $f_x^n$ , the stability proof follows along the same lines as above, to conclude that the origin of the closed loop system in the plane  $yz^n$  is asymptotically stable.

## D. Quadrotor attitude control

The proposed reactive force can be adapted to any vehicle with hover capability. For this work, we focus on a quadrotor. Different approaches for attitude control can be found in the literature, and most of them can be used with the reactive force proposed. For instance, defining  $\mathbf{f}^n = [f_x^n \ f_y^n \ f_z^n]^\top$ , the geometric approach in [19] can be constructed as

$$\mathbf{f}^n = \mathbf{R}_d \begin{bmatrix} 0 \\ 0 \\ T \end{bmatrix}$$

where  $T = \|\mathbf{f}^n\|$  is the thrust produced by the quadrotor's propellers, and  $\mathbf{R}_d$  is the rotation matrix that rotate from frame  $\mathcal{F}^b$  to  $\mathcal{F}^n$ . Thus, the problem is reduced to find  $\mathbf{R}_d$  that will be the reference for attitude control.

In this work we follow the approach set up in [9], where the attitude control for a quadrotor is proposed as

$$\tau^b = - \begin{bmatrix} 0 \\ 0 \\ 1 \end{bmatrix} \times (\mathbf{q}_{n,b}^* \otimes \mathbf{f}^n \otimes \mathbf{q}_{n,b}) - k_\Omega \Omega_{n,b}^b \quad (13)$$

where  $k_\Omega$  is a control gain and  $\mathbf{q}_{n,b}^*$  is the unit quaternion conjugate defined as  $\mathbf{q}_{n,b}^* = [q_0, -q_1, -q_2, -q_3]^\top$ . The term  $\mathbf{q}_{n,b}^* \otimes \mathbf{f}^n \otimes \mathbf{q}_{n,b}$  represents the transformation of  $\mathbf{f}^n$  to body axes  $\mathbf{f}^b$ . Additionally, it includes the cross product between the  $z^b$  axis and  $\mathbf{f}^b$  since the thrust in the quadrotor is always aligned with the  $z^b$  axis. The proposed reactive force  $\mathbf{f}^n$  is injected into the attitude system as torques. This is achieved by saturating the force  $\mathbf{f}^n$  with the saturation function

$$\tilde{\mathbf{f}}^n = \alpha \left( 1 - e^{k_f \|\mathbf{f}^n\|} \right) \frac{\mathbf{f}^n}{\sqrt{\|\mathbf{f}^n\|^2 + \Delta^2}} \quad (14)$$

where  $\Delta$  is a positive constant to avoid division by zero,  $\alpha$  represents the maximum torque the control vector can inject into the attitude system and  $k_f$  is a tuning parameter. Finally  $\mathbf{f}^n$  needs to be mapped to the actual thrust vector of the quadrotor. This can be done in several ways, but we use

$$T = \|\mathbf{f}^n\| \quad (15)$$

which guarantees that the total thrust is always positive. The stability proof is given in [9].

#### IV. PATH PLANNING (CUBIC SPLINES)

There are several methods to construct a cargo transportation path from an initial point  $\mathbf{X}_I$  to a final destination  $\mathbf{X}_F$ . These methods are basically an interpolation between the required points. This work's proposed method is based on cubic splines, which has interesting and powerful properties that give us a smooth continuous path.

A cubic spline is a piecewise polynomial function with maximum degree 3 [20], which takes values from an interval  $[x_i, x_{i+1}]$  and maps them to  $\mathbb{R}$ , i.e.

$$S : [x_i, x_n] \rightarrow \mathbb{R}$$

and it is composed of a piecewise polynomial function

$$S(x) = \begin{cases} s_1(x) & \forall [x_1, x_2] \\ s_2(x) & \forall [x_2, x_3] \\ \vdots & \\ s_{n-1}(x) & \forall [x_{n-1}, x_n] \end{cases}.$$

The cubic splines have the general form

$$s_i(x) = a_i + b_i(x-x_i) + c_i(x-x_i)^2 + d_i(x-x_i)^3 \quad (16)$$

and must satisfy the conditions

$$\begin{aligned} s_i(x_i) &= y_i, & i &= 1, \dots, n-1 \\ s_i(x_i) &= s_{i-1}(x_i) \\ \dot{s}_i(x_i) &= \dot{s}_{i-1}(x_i) \\ \ddot{s}_i(x_i) &= \ddot{s}_{i-1}(x_i) \\ \ddot{s}_0(x_i) &= \ddot{s}_{n-1}(x_n) = 0. \end{aligned}$$

which guarantees a smooth and continuous transition between splines. The proposed procedure to construct a spline that not lie in the planes  $xz^n$ ,  $yz^n$  or  $xy^n$  is described as follows:

- Given the initial  $\mathbf{X}_0 = [x_0 \ y_0 \ z_0]^\top$  and final  $\mathbf{X}_n = [x_n \ y_n \ z_n]^\top$  cargo destination, construct the line that join the two points.
- Define the line between  $\mathbf{X}_0$  and  $\mathbf{X}_n$  and the  $z^n$  axis to form a new plane  $pz^n$ , in which we will construct the desired path for the load.
- Express the coordinates  $x_0, y_0, x_n, y_n$  in terms of the new plane  $pz^n$ , such as

$$\begin{aligned} x_0^p &= \|[x_0 \ y_0]^\top\| \\ x_n^p &= \|[x_n \ y_n]^\top\| \end{aligned}$$

where  $[x_0^p \ z_0]^\top \in pz^n$  and  $[x_n^p \ z_n]^\top \in pz^n$ .

- Provide at least one desired altitude, called the safety altitude  $z_s$ . It is required at least one but we can chose several safety altitudes as we want  $z_s = [z_1 \ \dots \ z_{n-1}]$ .
- Compute the pair  $[x_s \ y_s]$  for every point given in  $z_s$  as

$$\begin{aligned} x_i &= \frac{x_n - x_0}{n-1} + x_{i-1} \\ y_i &= (y_n - y_0) \frac{x_i - x_0}{x_n - x_0} + y_0 \end{aligned}$$

with  $i = 1, \dots, n-1$ .

- Project the pair  $[x_s \ y_s]$  to the  $pz^n$  plane by

$$x_i^p = \|[x_i \ y_i]^\top\|.$$

- Compute the cubic spline that reaches the set of points  $\{[x_0 \ z_0], [x_i^p \ z_i], \dots, [x_{n-1}^p \ z_{n-1}], [x_n \ z_n]\}$ .
- Parameterize the spline  $S(x)$  in terms of time  $t$ . The parameterization can be solved in many different ways. Two of the them are:

- When  $d_i = 0$  in (16), we consider the parameterization

$$\begin{aligned} x_d^p &= ct \\ z_d &= a_i + b_i(ct - x_i) + c_i(ct - x_i)^2. \end{aligned}$$

- When  $d_i \neq 0$  in (16), we require a more complex parameterization

$$\begin{aligned} \dot{x}_d^p &= f(t) \\ z_d &= a_i + b_i(f(t) - x_i) + c_i(f(t) - x_i)^2. \end{aligned}$$

- Depending on the parameterization, compute  $x_d$  and  $y_d$  in terms of the inertial frame  $\mathcal{F}^n$  with

$$\begin{aligned} x_d &= \frac{x_n}{\|[x_n \ y_n]^\top\|} ct \\ y_d &= \frac{y_n}{\|[x_n \ y_n]^\top\|} ct \end{aligned}$$

or

$$\begin{aligned} \dot{x}_d &= \frac{x_n}{\|[x_n \ y_n]^\top\|} f(t) \\ \dot{y}_d &= \frac{y_n}{\|[x_n \ y_n]^\top\|} f(t) \end{aligned}$$

## V. SIMULATIONS

In this section, we present three simulation scenarios to show operational behaviour. First, we show how our solution can eliminate oscillations in the load. Second, cargo transportation from an initial position into different waypoints, and third, the path planning algorithm. The simulation parameters are summarized in Table I.

TABLE I  
SYSTEM PARAMETERS

Parameter	Value
$m_q$	1 kg
$m_l$	0.146 kg
$l$	0.65 m
$J_x$	0.04352 kg m <sup>2</sup>
$J_y$	0.04352 kg m <sup>2</sup>
$J_z$	0.07072 kg m <sup>2</sup>

### A. Scenario 1: Oscillation avoidance

The first simulation shows the ability to eliminate oscillations in the load, so we take the initial conditions in the most critical point when the load is just a little below the quadrotor, that is when  $r_3 \approx 0$ . Therefore, the initial conditions are

$$\begin{aligned}
 x_d &= 0; & y_d &= 0; & z_d &= 2 \\
 \mathbf{p}_1^n &= [0, 0, 1]^T \\
 \boldsymbol{\omega} &= [0, 0.2, 0]^T \\
 \mathbf{V}_1^n &= [0, 0, 0]^T \\
 \mathbf{r} &= \begin{bmatrix} \sin(1.56) \cos\left(\frac{\pi}{4}\right) \\ \sin(1.56) \sin\left(\frac{\pi}{4}\right) \\ -\cos(1.56) \end{bmatrix} \\
 \mathbf{q}_{n,b} &= [1, 0, 0, 0]^T \\
 \boldsymbol{\Omega}_{n,b}^b &= [0, 0, 0]^T.
 \end{aligned}$$

The gain parameters are chosen as  $k_{p_x} = -1.75$ ,  $k_{d_x} = -1.5$ ,  $k_{p_y} = -1.75$ ,  $k_{d_y} = -1.5$ ,  $k_{p_z} = -4$ ,  $k_{d_z} = -3$ ,  $k_w = -2$ .

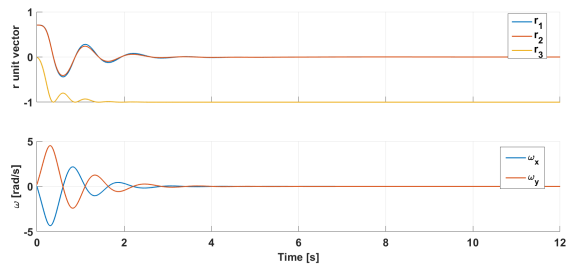


Fig. 4. Swing load position and velocity

Figure 4 shows how the load oscillation vanishes with the reactive force injected into the suspended load. It is desired

that  $r_1$  and  $r_2$  be small for cargo transportation, thus, it can be appreciated how  $r_1 \rightarrow 0$  and  $r_2 \rightarrow 0$  after four seconds. It is important to remark that the control proposed in this paper does not establish any control over the swing angles or any restriction over unit vector  $\mathbf{r}$ ; this fact permits to adapt a natural angular position in the load. Moreover, a damping term is introduced to control the angular velocity in the load oscillation, and we see in Figure 4 how the angular velocity of the load movement vanishes.

Besides, while the quadrotor compensates for the load oscillations, the load also moves to its desired position, as shown in Figure 5. Quadrotor thrust and cable tension can be observed in Figure 6. The cable tension was computed as in [1], using the identities  $T = T \mathbf{r} \cdot \mathbf{r}$ , where the quantity  $T \mathbf{r}$  is determined from  $m_l \dot{V}_{l_x}^n = T \mathbf{r} - m_l g \mathbf{e}_3$ .

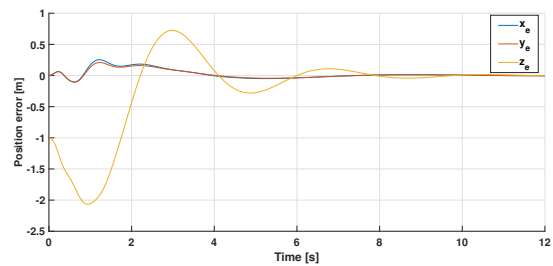


Fig. 5. Load position error

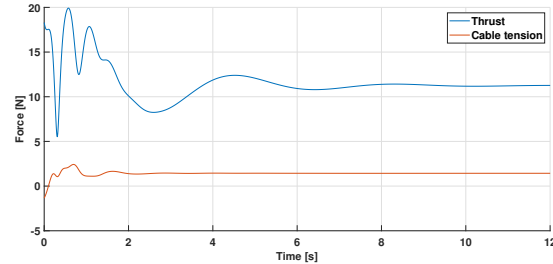


Fig. 6. Quadrotor thrust and cable tension

In Figure 7 the quadrotor handles the load oscillation rotation about  $x^b$  and  $y^b$  axes, and after the load oscillation vanishes the quadrotor maintain a hover flight such that  $q_0 = 1$  and  $[q_1, q_2, q_3] = 0$ .

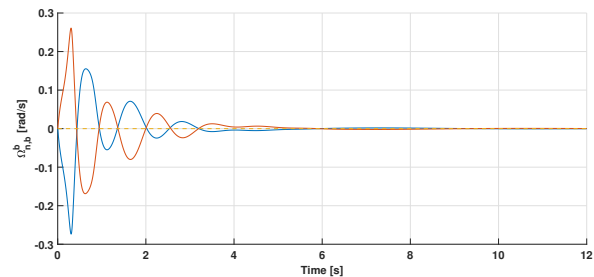


Fig. 7. Quadrotor attitude and angular velocities

Moreover, Figure 7 shows the quadrotor angular velocities to achieve the reactive forces directed by the control law. We end the first simulation scenario with torques produced by the quadrotor, shown in Figure 8. The values to set up the saturation function in (14) are  $\alpha = 3$ ,  $k_f = 1$  and  $\Delta = 0.001$ .

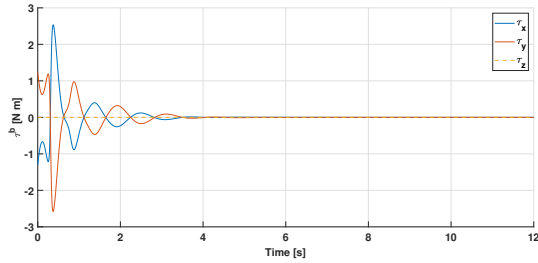


Fig. 8. Quadrotor's torques

### B. Scenario 2: Transporting cargo (waypoint)

For the second simulation scenario, a set of waypoints will be assigned as desired points for the load. The initial conditions are set in a suggested cargo transport situation as

$$x_d = [0, 20, -1]^T$$

$$y_d = [0, 10, 1]^T$$

$$z_d = [3, 5, 10]^T$$

$$\omega = [0, 0, 0]^T$$

$$\mathbf{p}_1^n = [0, 0, 1]^T$$

$$\mathbf{V}_1^n = [0, 0, 0]^T$$

$$\mathbf{r} = [0, 0, -1]^T$$

$$\mathbf{q}_{n,b} = [1, 0, 0, 0]^T$$

$$\mathbf{\Omega}_{n,b}^b = [0, 0, 0]^T$$

while the gains and saturation parameters are the same as in scenario 1. Figure 9 shows the quadrotor's load movement, showing how the load changes its position when the quadrotor starts moving. We notice that the quadrotor's initial abrupt movement entails an oscillation in the load, but the reactive force absorbs the swing movement after some seconds.

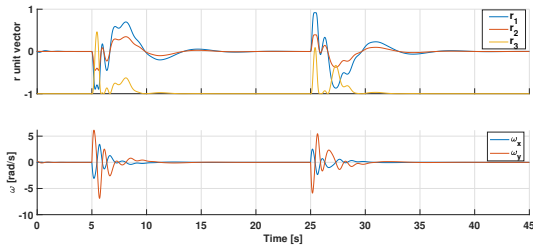


Fig. 9. Swing load attitude

The load position error converges to the origin, and the performance can be modified by changing the gains to inject more damping in the load to achieve a more soft approach

towards the waypoint, depending on task requirements. The quadrotor thrust and cable tension can be observed in Figure 11.

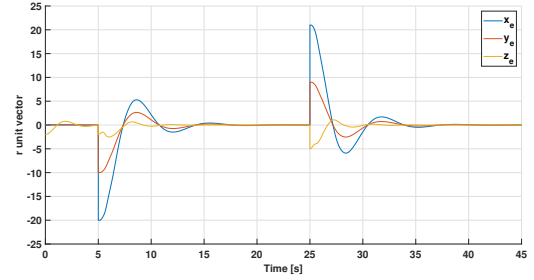


Fig. 10. Load position error

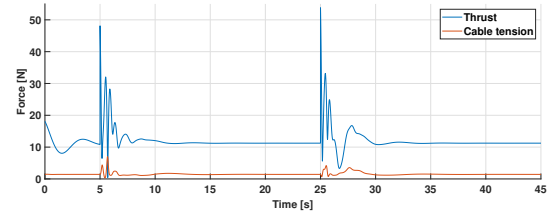


Fig. 11. Quadrotor thrust and cable tension

The quadrotor attitude and angular velocities are presented in Figure 12. We notice that after reaching a waypoint, the quadrotor passes to hover flight.

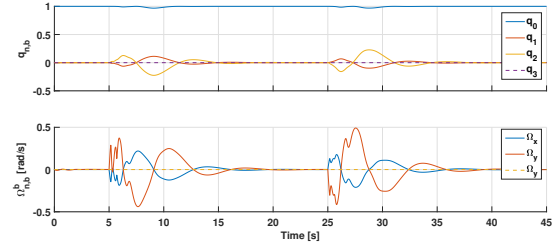


Fig. 12. Quadrotor attitude and angular velocities

### C. Scenario 3: Transporting cargo (path planning)

In this scenario we test the path planning strategy based on cubic splines. We select the initial and final points, as well as one safety altitude such as

$$\mathbf{X}_I = [0, 0, 0]^T \quad \text{Initial point}$$

$$\mathbf{X}_f = [15, -10, 3]^T \quad \text{Final point}$$

$$z_s = 12 \quad \text{Safety altitude}$$

and the resulting points in the plane of movement are

$$\mathbf{X}^P = [0, 8.412, 18.027]^T$$

$$\mathbf{Z}^P = [0, 12, 3].$$

The spline is further time-parameterized to define the desired path as

$$\begin{aligned} z_d &= c(k t)^2 + b k t \\ x_d &= \frac{15}{\sqrt{15^2 + 10^2}} k t \\ y_d &= -\frac{10}{\sqrt{15^2 + 10^2}} k t \end{aligned}$$

with  $b = 2.528$ ,  $c = -0.131$  and  $k = 0.1$ . We assume that the initial conditions are reasonably close to the initial point and defined as

$$\begin{aligned} \omega &= [0, 0, 0]^\top \\ \mathbf{p}_1^n &= [0, -1, -2]^\top \\ \mathbf{V}_1^n &= [0, 0, 0]^\top \\ \mathbf{r} &= [0, 0, -1]^\top \\ \mathbf{q}_{n,b} &= [1, 0, 0, 0]^\top \\ \Omega_{n,b}^b &= [0, 0, 0]^\top. \end{aligned}$$

Figure 13 shows the swing load attitude that converges towards zero. We notice a small jump at  $t = 180$  due to the transition between trajectory tracking and hover flight. Figure 14 shows the load position error that converges towards zero, and hence the load follows the desired path.

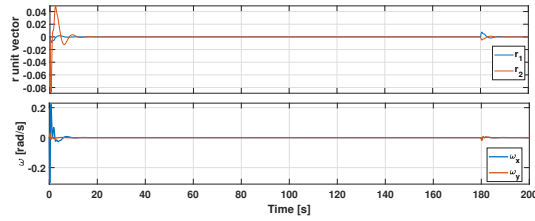


Fig. 13. Swing load attitude

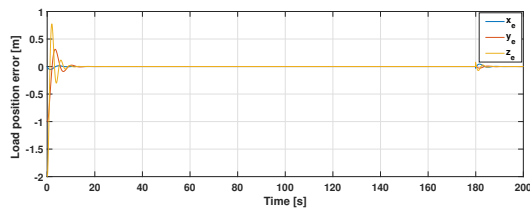


Fig. 14. Load position error

Finally, the movement of the load in inertial axes can be visualized better in Figure 15, where after 180 seconds, the load reach the final point and change to a hover flight.

## VI. CONCLUSIONS

This paper has presented a solution to swing attenuation and position control of a load suspended from a quadrotor based on reactive control. With this approach, we derive an easily implementable control algorithm, independent of the generation of desired swing angles. Asymptotic stability of the system's closed-loop equilibrium is proved using

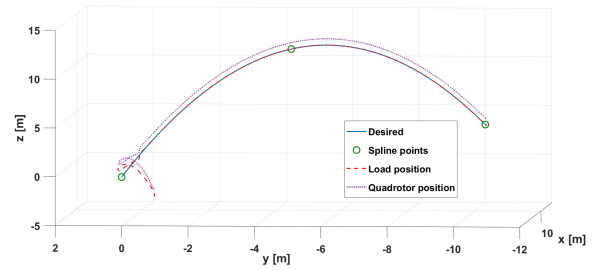


Fig. 15. Three-dimensional load path

Lyapunov theory. Also, a path planning strategy based on cubic splines was developed for three-dimensional space. The computed desired path is converted to a trajectory with the correct parameterization, where the reactive force enables trajectory tracking. Finally, we have demonstrated the control law and path planning approach performance through three simulated scenarios, including reducing load oscillations and load transportation through different waypoints and trajectory tracking of the spline. Our future work will be testing the control approach in lab experiments.

## APPENDIX

The matrix  $A$  of (10) needs to be Hurwitz for the Lyapunov proof to hold. The eigenvalues of  $A$  are

$$\text{eig}(A) = \begin{bmatrix} r_3^2 k_{d_z} \pm |r_3| \sqrt{k_{d_z}^2 r_3^2 + 4 k_{p_z}} \\ k_{d_x} \pm \sqrt{k_{d_x}^2 + 4 k_{p_x}} \\ |r_3| 2 k_\omega m_t \end{bmatrix}.$$

From the first pair of eigenvalues  $k_{d_z} < 0$  and

$$r_3^2 |k_{d_z}| > |r_3| \sqrt{k_{d_z}^2 r_3^2 + 4 k_{p_z}}$$

thus  $k_{p_z} < 0$ . The second pair of eigenvalues give us a similar solution  $k_{p_x} < 0$  and  $k_{d_x} < 0$ . Finally from the last eigenvalue  $k_\omega < 0$ . Therefore the Hurwitz condition is satisfied with  $[k_{p_x}, k_{d_x}, k_{p_z}, k_{d_z}, k_\omega] < 0$ .

## REFERENCES

- [1] K. Sreenath, N. Michael, and V. Kumar, "Trajectory generation and control of a quadrotor with a cable-suspended load—a differentially-flat hybrid system," in *Proceedings of International Conference on Robotics and Automation*. IEEE, 2013, pp. 4888–4895.
- [2] M. E. Guerrero-Sánchez, D. A. Mercado-Ravell, R. Lozano, and C. D. García-Beltrán, "Swing-attenuation for a quadrotor transporting a cable-suspended payload," *ISA transactions*, vol. 68, pp. 433–449, 2017.
- [3] S. Sadr, S. A. A. Moosavian, and P. Zarfshan, "Dynamics modeling and control of a quadrotor with swing load," *Journal of Robotics*, vol. 2014.
- [4] M. E. Guerrero, D. Mercado, R. Lozano, and C. García, "Passivity based control for a quadrotor UAV transporting a cable-suspended payload with minimum swing," in *Proceedings of 54th Conference on Decision and Control (CDC)*. IEEE, 2015, pp. 6718–6723.
- [5] K. Klausen, T. I. Fossen, and T. A. Johansen, "Nonlinear control of a multirotor uav with suspended load," in *Proceedings International Conference on Unmanned Aircraft Systems (ICUAS)*. IEEE, 2015, pp. 176–184.
- [6] O. Egeland and J. T. Gravdahl, *Modeling and simulation for automatic control*. Marine Cybernetics Trondheim, Norway, 2002.

- [7] D. Cabecinhas, R. Cunha, and C. Silvestre, "A trajectory tracking control law for a quadrotor with slung load," *Automatica*, vol. 106, pp. 384–389, 2019.
- [8] A. Paz-Mosco, R. Castro-Linares, and H. Rodríguez-Cortés, "Trajectory tracking control for a quadrotor with a slung load," in *Proceedings International Conference on Unmanned Aircraft Systems (ICUAS)*. IEEE, 2020.
- [9] T. S. Andersen and R. Kristiansen, "Reactive-based position control of and underactuated quadrotor," in *Proceedings of European Control Conference (ECC)*. IEEE, 2020, pp. 1656–1661.
- [10] A. Sánchez, V. Parra-Vega, C. Tang, F. Oliva-Palomo, and C. Izaguirre-Espinosa, "Continuous reactive-based position-attitude control of quadrotors," in *Proceedings of American Control Conference (ACC)*. IEEE, 2012, pp. 4643–4648.
- [11] P. Sujit, S. Saripalli, and J. B. Sousa, "Unmanned aerial vehicle path following: A survey and analysis of algorithms for fixed-wing unmanned aerial vehicles," *IEEE Control Systems Magazine*, vol. 34, no. 1, pp. 42–59, 2014.
- [12] M. Breivik and T. I. Fossen, "Principles of guidance-based path following in 2D and 3d," in *Proceedings of the 44th IEEE Conference on Decision and Control*.
- [13] S. Fielding and M. Nahon, "Input shaped trajectory generation and controller design for a quadrotor-slung load system," in *2019 International Conference on Unmanned Aircraft Systems (ICUAS)*. IEEE, 2019, pp. 162–170.
- [14] B. Sun, H. Chaofang, L. Cao, N. Wang, and Y. Zhou, "Trajectory planning of quadrotor uav with suspended payload based on predictive control," in *2018 37th Chinese Control Conference (CCC)*. IEEE, 2018, pp. 10 049–10 054.
- [15] T. S. Andersen and R. Kristiansen, "Quaternion path-following in three dimensions for a fixed-wing UAV using quaternion blending," in *2018 IEEE Conference on Control Technology and Applications (CCTA)*. IEEE, 2018, pp. 1597–1602.
- [16] H. Goldstein, C. Poole, and J. Safko, "Classical mechanics," 2002.
- [17] T. S. Andersen and R. Kristiansen, "Quaternion guidance and control of quadrotor," in *Proceedings of International Conference on Unmanned Aircraft Systems (ICUAS)*. IEEE, 2017, pp. 1567–1601.
- [18] H. K. Khalil and J. W. Grizzle, *Nonlinear systems*. Prentice hall Upper Saddle River, NJ, 2002, vol. 3.
- [19] T. Lee, M. Leok, and N. H. McClamroch, "Geometric tracking control of a quadrotor UAV on SE (3)," in *49th IEEE conference on decision and control (CDC)*. IEEE, 2010, pp. 5420–5425.
- [20] C. De Boor and C. De Boor, *A practical guide to splines*. springer-verlag New York, 1978, vol. 27.